

## Critical role of water conditions in the responses of autumn phenology of marsh wetlands to climate change on the Tibetan Plateau

Shen, Xiangjin; Shen, Miaogen; Wu, Chaoyang; Peñuelas, Josep; Ciais, Philippe; Zhang, Jiaqi; Freeman, Chris; Palmer, Paul I.; Liu, Binhui; Henderson, Mark; Song, Zhaoliang; Sun, Shaobo; Lu, Xianguo; Jiang, Ming

### Global Change Biology

DOI:  
[10.1111/gcb.17097](https://doi.org/10.1111/gcb.17097)

Published: 01/01/2024

Peer reviewed version

[Cyswllt i'r cyhoeddiad / Link to publication](#)

#### *Dyfyniad o'r fersiwn a gyhoeddwyd / Citation for published version (APA):*

Shen, X., Shen, M., Wu, C., Peñuelas, J., Ciais, P., Zhang, J., Freeman, C., Palmer, P. I., Liu, B., Henderson, M., Song, Z., Sun, S., Lu, X., & Jiang, M. (2024). Critical role of water conditions in the responses of autumn phenology of marsh wetlands to climate change on the Tibetan Plateau. *Global Change Biology*, 30(1), Article e17097. <https://doi.org/10.1111/gcb.17097>

#### **Hawliau Cyffredinol / General rights**

Copyright and moral rights for the publications made accessible in the public portal are retained by the authors and/or other copyright owners and it is a condition of accessing publications that users recognise and abide by the legal requirements associated with these rights.

- Users may download and print one copy of any publication from the public portal for the purpose of private study or research.
- You may not further distribute the material or use it for any profit-making activity or commercial gain
- You may freely distribute the URL identifying the publication in the public portal ?

#### **Take down policy**

If you believe that this document breaches copyright please contact us providing details, and we will remove access to the work immediately and investigate your claim.

1 **Critical role of water conditions in the responses of autumn phenology**  
2 **of marsh wetlands to climate change on the Tibetan Plateau**

3 Xiangjin Shen<sup>1</sup>, Miaogen Shen<sup>2</sup>, Chaoyang Wu<sup>3</sup>, Josep Peñuelas<sup>4,5</sup>, Philippe Ciais<sup>6</sup>,  
4 Jiaqi Zhang<sup>1,7</sup>, Chris Freeman<sup>8</sup>, Paul I. Palmer<sup>9,10</sup>, Binhui Liu<sup>11</sup>, Mark Henderson<sup>12</sup>,  
5 Zhaoliang Song<sup>13</sup>, Shaobo Sun<sup>13</sup>, Xianguo Lu<sup>1</sup>, Ming Jiang<sup>1\*</sup>

6 <sup>1</sup>Northeast Institute of Geography and Agroecology, Chinese Academy of Sciences,  
7 Changchun, China.

8 <sup>2</sup>State Key Laboratory of Earth Surface Processes and Resource Ecology, Faculty of  
9 Geographical Science, Beijing Normal University, Beijing, China.

10 <sup>3</sup>Institute of Geographic Sciences and Natural Resources Research, Chinese Academy  
11 of Sciences, Beijing, China.

12 <sup>4</sup>CREAF, Cerdanyola del Vallès, Barcelona, Spain.

13 <sup>5</sup>CSIC, Global Ecology Unit CREAF-CSIC- UAB, Barcelona, Spain.

14 <sup>6</sup>Laboratoire des Sciences du Climat et de l'Environnement, LSCE/IPSL,  
15 CEA-CNRS-UVSQ, Université Paris-Saclay, Gif-sur-Yvette, France.

16 <sup>7</sup>University of Chinese Academy of Sciences, Beijing, China.

17 <sup>8</sup>School of Natural Sciences, Bangor University, Bangor, UK.

18 <sup>9</sup>School of GeoSciences, University of Edinburgh, Edinburgh, UK.

19 <sup>10</sup>National Centre for Earth Observation, University of Edinburgh, Edinburgh, UK.

20 <sup>11</sup>College of Forestry, Northeast Forestry University, Harbin, China.

21 <sup>12</sup>Mills College, Northeastern University, Oakland, California, USA.

22 <sup>13</sup>Institute of Surface-Earth System Science, School of Earth System Science, Tianjin  
23 University, Tianjin, China.

24 **Correspondence:** Ming Jiang, Northeast Institute of Geography and Agroecology,  
25 Chinese Academy of Sciences, Changchun, China.

26 Email: jiangm@iga.ac.cn

27 **Abstract:** The Tibetan Plateau, housing 20% of China's wetlands, plays a vital role in  
28 the regional carbon cycle. Examining the phenological dynamics of wetland vegetation  
29 in response to climate change is crucial for understanding its impact on the ecosystem.  
30 Despite this importance, the specific effects of climate change on wetland vegetation  
31 phenology in this region remain uncertain. In this study, we investigated the influence of  
32 climate change on the end of the growing season (EOS) of marsh wetland vegetation  
33 across the Tibetan Plateau, utilizing satellite-derived Normalized Difference Vegetation  
34 Index (NDVI) data and observational climate data. We observed that the regionally  
35 averaged EOS of marsh vegetation across the Tibetan Plateau was significantly ( $P <$   
36  $0.05$ ) delayed by 4.10 days/decade from 2001 to 2020. Warming pre-season temperatures  
37 were found to be the primary driver behind the delay in the EOS of marsh vegetation,  
38 whereas pre-season cumulative precipitation showed no significant impact. Interestingly,  
39 the responses of EOS to climate change varied spatially across the plateau, indicating a  
40 regulatory role for hydrological conditions in marsh phenology. In the humid and cold  
41 central regions, pre-season daytime warming significantly delayed the EOS. However,  
42 areas with lower soil moisture exhibited a weaker or reversed delay effect, suggesting  
43 complex interplays between temperature, soil moisture, and EOS. Notably, in the arid  
44 southwestern regions of the plateau, increased pre-season rainfall directly delayed the  
45 EOS, while higher daytime temperatures advanced it. Our results emphasize the critical  
46 role of hydrological conditions, specifically soil moisture, in shaping marsh EOS  
47 responses in different regions. Our findings underscore the need to incorporate

48 hydrological factors into terrestrial ecosystem models, particularly in cold and dry  
49 regions, for accurate predictions of marsh vegetation phenological responses to climate  
50 change. This understanding is vital for informed conservation and management  
51 strategies in the face of current and future climate challenges.

52

53 **KEYWORDS** marsh wetlands, vegetation, autumn phenology, climate change, water  
54 condition, Tibetan Plateau

55

## 56 **1 Introduction**

57 Vegetation phenology refers to the seasonal timing of life cycle events in plants and  
58 reflects the dynamic responses of terrestrial ecosystems to global climate change (Chen  
59 et al., 2017; Peñuelas et al., 2001; Piao et al., 2007, 2008, 2019; Richardson et al., 2013;  
60 Wu et al., 2022). Several studies have demonstrated that autumn phenology, signaling  
61 the end of the growing season (EOS), reflects the vegetation's growing period better  
62 than spring phenology and has a significant effect on carbon sequestration in terrestrial  
63 ecosystems (Bao et al., 2020; Fu et al., 2018; Garonna et al., 2014; Zhu et al., 2012).

64 Global climate change has significantly changed the autumn phenology worldwide,  
65 affecting the regional and global energy balance, water flux, and carbon budget (Che et  
66 al., 2014; Estiarte et al., 2015; Kelsey et al., 2021; Richardson et al., 2013; Yang et al.,  
67 2021). Although the variations in the autumn phenology of vegetation and its response  
68 to regional and global climate changes have been extensively analyzed, most studies

69 have focused on grassland or forest ecosystems, with few investigations of wetland  
70 ecosystems (Coleman et al., 2022; Ge et al., 2015; Ma et al., 2022; Rice et al., 2018;  
71 Yang et al., 2015). Due to the unique environmental conditions in wetlands, climate  
72 change may have different effects on the autumn phenology of vegetation compared to  
73 other ecosystems (Keppeler et al., 2021; Ma et al., 2022; Molino et al., 2022; Shen,  
74 Wang, et al., 2022). Such differences must be considered if we are to better understand  
75 the responses of the global carbon cycle and ecosystem vegetation to climatic variation  
76 in the context of global climate change.

77 As the highest plateau in the world, the Tibetan Plateau is highly sensitive to  
78 climate change. And yet the roles of temperature or precipitation in determining the  
79 vegetation phenology of the Tibetan Plateau appear contradictory; Some studies assert  
80 that temperature plays a dominant role in determining vegetation phenology (Yu et al.,  
81 2010), while others argue that precipitation is critical to the vegetation phenology of the  
82 region (Shen et al., 2014; Shen, Piao, Cong, et al., 2015). Known as the “water tower of  
83 Asia”, the Tibetan Plateau features a large area of marsh wetlands with relatively high  
84 water content (Che et al., 2014; Shen et al., 2011; Shen, Jiang, et al., 2021) that provide  
85 an ideal opportunity for clarifying the dominant effects of temperature and precipitation  
86 on the phenology of the vegetation of the Tibetan Plateau.

87 Recent studies have analyzed the effects of climate change on autumn phenology  
88 in various ecosystems of the region (Shen, Wang, et al., 2022), reported the phenology  
89 of grassland vegetation as positively correlated with precipitation and negatively

90 correlated with daytime maximum temperature. Increased precipitation can enhance the  
91 water use efficiency of grassland vegetation, potentially delaying the EOS (Shen, Piao,  
92 Dorji, et al., 2015; Wu et al., 2018). However, an increase in daytime maximum  
93 temperature also promotes evaporation, reducing water use efficiency and consequently  
94 advancing the EOS. Clearly, an improved understanding of the influence of climate  
95 variation on the autumn phenology of marsh vegetation in this region can greatly  
96 improve our knowledge of the relationships between the vegetation of ecosystems and  
97 climate change.

98 This study utilizes data from 2001 to 2020, incorporating the Normalized  
99 Difference Vegetation Index (NDVI) and observational climate data, to explore  
100 spatiotemporal variations in the end of the growing season (EOS) and their responses to  
101 climatic variations in the marshes of the Tibetan Plateau. The objective is to enhance  
102 our understanding and predictive capabilities regarding phenological changes in marsh  
103 vegetation. By illuminating the intricate relationship between vegetation and climate  
104 change in this ecologically significant area, the findings of our study can offer valuable  
105 new insights for ecological management and conservation efforts.

106

## 107 **2 Material and method**

### 108 2.1 Study region

109 The Tibetan Plateau is located in southwestern China at an altitude of 3,000–5,000 m  
110 (average altitude > 4,000 m) and is characterized by a semi-arid and cold climate

111 (Figure 1) (Shen, Liu, et al., 2022). The annual precipitation exceeds 1,000mm in the  
112 southeastern region and is < 100mm in the northwestern region (Cheng et al., 2021; Gao  
113 et al., 2013). The average temperature in the northwestern and southeastern areas is  
114 approximately  $-6^{\circ}\text{C}$  and  $20^{\circ}\text{C}$ , respectively (Qin et al., 2022).

115 As the highest plateau in the world, the Tibetan Plateau is extremely sensitive to  
116 climate change (Dong et al., 2012; Zhang et al., 2013). Changes in vegetation  
117 phenology in this region serve as crucial indicators of global climate change (Chen et al.,  
118 2015). Large wetland areas characterized by marshes are distributed on the Tibetan  
119 Plateau and are important for the ecological security of the region and the major river  
120 systems that originate there, including the Yangtze, Yellow, and Lancang rivers (Liu et  
121 al., 2021; Shen et al., 2023). The main species of marsh plants distributed on the Tibetan  
122 Plateau are *Phragmites australis*, *Blysmus sinocompressus*, *Carex pseudosupina*, and  
123 *Kobresia littledalei* (Shen, Jiang, et al., 2021).

124

## 125 2.2 Data

126 Satellite-derived NDVI data covering the 2001–2020 period were obtained from the  
127 MOD13Q1 NDVI dataset, with temporal and spatial resolutions of 16 d and 250 m,  
128 respectively (Shen et al., 2023). This dataset was provided by the Earth Science Data  
129 Systems of the National Aeronautics and Space Administration.

130 The distribution of marshes in the study area was obtained from the wetland  
131 distribution datasets for China for years 2000 and 2015 at a resolution of  $30\text{ m} \times 30\text{ m}$

132 (Mao et al., 2020). These digital maps were available from the National Earth System  
133 Science Data Center. The accuracy of datasets had been verified through field  
134 observations, and the producer's and user's accuracies were over 95% and 98%,  
135 respectively (Mao et al., 2020). In order to exclude the impact of land use or cover  
136 change on the results, we used the marsh distribution data for two specific years (2000  
137 and 2015) to extract the unchanged marsh distribution as the study area (Shen et al.,  
138 2023).

139 The soil moisture data used in this study were extracted from a 1-km daily soil  
140 moisture dataset of in situ measurements conducted in China from 2001 to 2020 (Li et  
141 al., 2022). These dataset was produced using spatially dense in situ observations and  
142 machine learning, and was obtained from the National Tibetan Plateau Scientific Data  
143 Center.

144 The Climate Change Research Center of the Chinese Academy of Sciences  
145 provided the daily gridded climate data from more than 2400 meteorological stations  
146 distributed across China. These included daily precipitation as well as the minimum,  
147 maximum, and mean temperatures with a spatial resolution of 1 km from 2001 to 2020.  
148 Marsh distribution, soil moisture, and climatic data were resampled at a resolution of  
149  $250\text{ m} \times 250\text{ m}$  to maintain consistency with the spatial resolution of the NDVI data  
150 (Shen, Liu, et al., 2021).

151

152 2.3 Methods



153 Considering that snow cover decreases the NDVI value, consequently affecting the  
154 accuracy of satellite-derived phenology data, we replaced the snow-contaminated NDVI  
155 values with the median value of the uncontaminated winter NDVI values between  
156 November and the following March for each pixel (Shen et al., 2014; Shen, Piao, Cong,  
157 et al., 2015). This preprocessing of data has been validated and included in numerous  
158 previous studies (Ganguly et al., 2010; Shen, Piao, Cong, et al., 2015; Wang et al.,  
159 2021). In addition, we removed the pixels with long-term (2001-2020) mean NDVI  
160 averaged from May to September  $\leq 0$  to exclude the impact of non-vegetation pixels on  
161 the results (Shen, Jiang, et al., 2021). In general, with increasing Julian day, the NDVI  
162 value for a vegetation pixel gradually increases and then declines after reaching its  
163 maximum. Consistent with many previous studies (e.g. Ma et al., 2022; Piao et al., 2011;  
164 Shen et al., 2018, 2019; Su et al., 2022; Wu & Liu, 2013; Zhang et al., 2013), this study  
165 used the Polyfit-Maximum method (Piao et al., 2006, 2011) to represent the seasonal  
166 changes in NDVI as a function of Julian day and extract phenological information.  
167 Because of the impact of some nonvegetation effects of cloud, atmosphere, solar zenith  
168 angle, and other factors, some NDVI values are lower than their two adjacent ones.  
169 Evidently, the polynomial function fitting a smooth NDVI seasonal curve as a function  
170 of time can help smooth these abnormal values (Piao et al., 2006; 2011). For the  
171 Polyfit-Maximum method, it is proved that a sixth-degree polynomial function is better  
172 to fit the NDVI time series and applicable in most cases (Kafaki et al., 2009; Piao et al.,  
173 2006, 2011; Su et al., 2022; Yang et al., 2015). This method has been demonstrated to be

174 capable of depicting the seasonal patterns of NDVI time series in northern mid and high  
175 latitudes well (e.g. Jeong et al., 2011; White et al., 2009; Wu & Liu, 2013). It is  
176 generally considered that the end date of growing season represents the period when  
177 vegetation growth begins to decline rapidly (Lee et al., 2002; Reed et al., 1994; Yu et al.,  
178 2003; Zhang et al., 2003). This date indicates when the NDVI annual cycle transitions  
179 from one stage to another, and this transition date corresponds to the times at which the  
180 rate of change in curvature in the NDVI shows local maximums (Piao et al., 2006;  
181 Zhang et al., 2003). Therefore, in the Polyfit-Maximum approach, the EOS date is set to  
182 correspond to the time of the largest decrease in NDVI at the end of the growth period  
183 (Piao et al., 2006). The Polyfit-Maximum method has been widely used to extract  
184 vegetation phenology owing to its excellent performance (e.g. Cong et al., 2013; Fu et  
185 al., 2014; Jeong et al., 2011; Kafaki et al., 2009; Li et al., 2023; Liu et al., 2016; Liu et  
186 al., 2023; Ma et al., 2022; Piao et al., 2015; Shen et al., 2018, 2019, 2023; Su et al.,  
187 2022; Wang et al., 2016; Wang et al., 2018; Wu & Liu, 2013; Yang et al., 2015; Yang et  
188 al., 2021; Zhang et al., 2013; Zhou et al., 2020) and consists in a number of steps.

189 First, we calculated the annual and multiyear average rates of NDVI variation to  
190 obtain the corresponding day of the year (DOY) for the vegetation's EOS (Piao et al.,  
191 2006). The following equation was used to calculate the rate of NDVI variation:

$$192 \quad \text{NDVI}_{\text{ratio}}(t) = \frac{\text{NDVI}(t+1) - \text{NDVI}(t)}{\text{NDVI}(t)} \quad (1)$$

193 where  $t$  is time (temporal resolution of 16 days),  $\text{NDVI}_{\text{ratio}}(t)$  is the rate of NDVI  
194 change corresponding to period  $t$ ,  $\text{NDVI}(t)$  is the NDVI value for period  $t$ , and

195 NDVI(t+1) is the NDVI value for period t+1. We detected the time t with the minimum  
 196  $NDVI_{ratio}$  and used the corresponding NDVI(t+1) at time (t+1) as the NDVI threshold  
 197 for the EOS.

198 Then, we used the maximum value method of multivariate fitting to construct a  
 199 unary sixth-degree polynomial function (Piao et al., 2006) and fitted the annual and  
 200 multiyear average daily NDVI fitting curve by pixel. The formula used was:

$$201 \quad NDVI = a + a_1x^1 + a_2x^2 + a_3x^3 + a_4x^4 + a_5x^5 + a_6x^6 \quad (2)$$

202 where x is the day of each year (DOY); and  $a_1, a_2, a_3, \dots, a_6$  are the regression  
 203 coefficients determined by least-squares regression.

204 Finally, we substituted the DOY into the fitting curve of the multiyear average  
 205 daily NDVI to obtain the NDVI threshold corresponding to the EOS (Piao et al., 2006).  
 206 We applied the NDVI threshold values to the daily NDVI fitting curve of each year to  
 207 obtain the corresponding EOS values for marsh vegetation in that year.

208 To analyze the EOS trend and climatic variables on the Tibetan Plateau from 2001  
 209 to 2020, we performed a linear regression analysis using the following equation (Piao et  
 210 al., 2011):

$$211 \quad \theta_{slope} = \frac{(n \times \sum_{i=1}^n i \times x_i) - (\sum_{i=1}^n i \sum_{i=1}^n x_i)}{n \times \sum_{i=1}^n i^2 - (\sum_{i=1}^n i)^2} \quad (3)$$

212 where  $n$  is the number of years analyzed (i.e., 20 years for this study);  $\theta_{slope}$   
 213 indicates the trend of the EOS (or climatic variable) for each pixel; and  $x_i$  is the EOS (or  
 214 climatic variable) during the  $i$  year. A negative  $\theta_{slope}$  implies that the temporal variation  
 215 shows an advancing (or a decreasing) trend, whereas a positive  $\theta_{slope}$  implies a delaying

216 (or increasing) trend.

217 To investigate the seasonal changes in the EOS in response to climate variations,  
218 we analyzed the simple correlation coefficients between monthly and seasonal climate  
219 factors and the EOS in previous winter (November to February of the following year),  
220 spring (March to May), summer (June to August), and autumn (September to October).  
221 In addition, we carried out a partial correlation analysis to further examine correlations  
222 between climate variables and the EOS. Through this analysis, it was possible to  
223 determine the relationship between two parameters after removing the influence of other  
224 factors (Peng et al., 2013; Shen et al., 2016).

225 The partial correlation coefficient between the time series of the EOS and daytime  
226 maximum temperature (or nighttime minimum temperature) was calculated to assess the  
227 effect of maximum temperature (or minimum temperature) on the EOS, with  
228 precipitation and minimum temperature (or maximum temperature) as the controlling  
229 variables. In line with previous studies, the duration of the preseason was calculated for  
230 the maximum temperature (or minimum temperature) based on the period preceding the  
231 long-term average date of the EOS. When the maximum temperature (or minimum  
232 temperature) had the highest absolute value for the partial correlation coefficient with  
233 the EOS, this period is referred to as the preseason for the maximum temperature (or the  
234 minimum temperature) (Shen et al., 2016; Wu et al., 2018). In this study, an interval of  
235 10 days was adopted to determine the duration of the preseason period and smooth out  
236 potential extreme values (Shen, Piao, Cong, et al., 2015).

237 The effect of preseason cumulative precipitation on the EOS was similarly  
238 analyzed, and preseason precipitation was determined by setting the maximum and  
239 minimum temperatures as the controlling variables (Shen et al., 2016). We did not  
240 constrain the duration of preseason precipitation to be equal to that of preseason  
241 temperature. In addition, to further analyze the influences of climatic variations on the  
242 EOS, we compared the partial correlation coefficients between the EOS and preseason  
243 precipitation and between the EOS and maximum and minimum temperatures at  
244 different levels of temperature and soil moisture.

245

### 246 **3 Results**

#### 247 3.1 Spatial and temporal variations in the EOS

248 The multiyear mean EOS on the Tibetan Plateau occurred primarily between 260th and  
249 300th day of year (DOY), with a regional average of 277th DOY (October 4, or October  
250 3 in leap years) (Figure 1b). The EOS was later in the low altitude (below 4,000 m)  
251 humid areas of the eastern Tibetan Plateau and earlier in the high-altitude (above 4,000  
252 m) central areas (Figure 1a,b).

253 The regionally averaged EOS from 2001 to 2020 across the Tibetan Plateau  
254 exhibited a significant delay of 4.10 days per decade ( $P < 0.05$ ) (Figure 1d). The  
255 percentage of pixels showing a trend of delayed EOS (68.5%, with a significant  
256 proportion of 36.2%,  $P < 0.05$ ) was higher than that showing a trend of advanced EOS  
257 (31.5%, with a significant proportion of 6.4%,  $P < 0.05$ ). The former trend was more

258 evident in the northern and western (high altitude permafrost areas) of the Tibetan  
259 Plateau, while the latter was concentrated in the central regions (Figure 1a,c).

260

### 261 3.2 Relationships between the EOS and climate variables

262 We first analyzed partial correlations between seasonal climate variables and the EOS  
263 without using pre-seasons. In autumn, the EOS showed a significant positive correlation  
264 with temperatures ( $P < 0.05$ ) but a weak negative correlation with precipitation ( $P >$   
265  $0.05$ ) across the Tibetan Plateau (Figure S1). The partial correlations between EOS and  
266 climatic variables in other seasons were not statistically significant ( $P > 0.05$ ).

267 We further analyzed the partial correlations between EOS and pre-season climatic  
268 variables. Across the Tibetan Plateau, the regionally averaged EOS showed a weak  
269 negative correlation with pre-season cumulative precipitation but a significant positive  
270 correlation with pre-season maximum and minimum temperatures (Figure 2). Spatially,  
271 the proportion of pixels displaying a negative correlation between EOS and pre-season  
272 cumulative precipitation was approximately 52.1%, and that with a significant negative  
273 relationship was approximately 7.6% (Figure 3a). The proportions of pixels showing a  
274 positive relationship between EOS and pre-season maximum and minimum temperatures  
275 were approximately 65.2% and 89.4%, respectively, and the proportions of pixels with a  
276 significant ( $P < 0.05$ ) positive relationship were 19.5% and 34.0%, respectively (Figure  
277 3c,e).

278

279 The partial correlations between EOS and pre-season climatic variables indicated  
280 spatial heterogeneity across the Tibetan Plateau. In the southwestern region, the EOS  
281 showed a positive and negative partial correlation with pre-season cumulative  
282 precipitation and pre-season maximum temperature, respectively; however, in the central  
283 area, it exhibited a significant negative and positive partial correlation with these two  
284 parameters, respectively (Figures 2, 3a,c). The partial relationships between EOS and  
285 pre-season minimum temperature were positive in most of the study area, and the  
286 positive relationships were extremely significant ( $P < 0.01$ ) in the western and eastern  
287 regions (Figure 3e).

288 Subsequently, we examined the partial correlations between EOS and pre-season  
289 climatic variables under different soil moisture levels in the study region (Figure 3). The  
290 results showed that as the pre-season soil moisture increased, the positive relationships  
291 between EOS and pre-season cumulative precipitation gradually weakened, whereas  
292 those between EOS and pre-season maximum and minimum temperatures became  
293 gradually stronger (Figures 3 and 4).

294

## 295 **4 Discussions**

### 296 4.1 Autumn phenology of marsh vegetation on the Tibetan Plateau

297 The long-term average EOS for marsh vegetation occurred later in the eastern Tibetan  
298 Plateau than in the central and southwestern regions (Figure 1b). This aligns with  
299 observations that the eastern area has a lower altitude and a warmer climate (Shen, Liu,

300 et al., 2021), thus allowing the growing season to continue for longer. This result is  
301 consistent with the findings of (Liu et al., 2021), which showed that the combined EOS  
302 for all vegetation types occurred earlier in the central Tibetan Plateau and later in the  
303 eastern regions. From 2001 to 2020, the average EOS was delayed by 4.10 days per  
304 decade across the plateau (Figure 1c), a trend consistent with the results of Shen et al.  
305 (Shen, Wang, et al., 2022), which showed a total delay of 8.2 days in the EOS for  
306 vegetation on the plateau over the same period.

#### 307 4.2 Climatic effects on the regionally averaged EOS for marsh vegetation

308 The regionally averaged EOS exhibited significant positive partial correlations with  
309 preseason daytime maximum and nighttime minimum temperatures but a weak negative  
310 correlation with preseason cumulative precipitation across the Tibetan Plateau. The  
311 phenology of marsh vegetation on the plateau observed in this study differed from that  
312 of grasslands reported in previous studies (Dorji et al., 2013; Shen, Wang, et al., 2022;  
313 Yang et al., 2021).

314 Previous studies have shown that in the grassland vegetation of the Tibetan Plateau,  
315 increased precipitation significantly enhances water use efficiency (Lin et al., 2020;  
316 Zhou et al., 2020), delaying the EOS. In these relatively arid systems, the higher  
317 maximum temperatures increase evaporation and reduce water use efficiency, thus  
318 advancing the EOS (Dorji et al., 2013; Yang et al., 2021). In contrast, the marshes  
319 examined in the present study contained far more water (Ganjurjav et al., 2022; Shen,  
320 Liu, et al., 2022), making it less likely that preseason precipitation would affect the



321 regionally averaged EOS for their vegetation, and explain how the abundance of water  
322 allowed the EOS to be delayed by the increased pre-season temperatures on the Tibetan  
323 Plateau.

324 Our results indicate that pre-season temperature is a key factor affecting the EOS,  
325 and an increase in this parameter significantly delayed the EOS on the Tibetan Plateau  
326 (Figure 3). It is known that increased pre-season maximum temperature can promote  
327 photosynthesis by enhancing the daytime photosynthetic activity of enzymes (Piao et al.,  
328 2007; Turnbull et al., 2022). This increased photosynthesis, together with raised  
329 nighttime minimum temperatures that reduce frost and low-temperature constraints  
330 (Shen et al., 2016), would further delay the EOS on the plateau.

331

#### 332 4.3 Elucidating spatial variations in the effects of climatic change on the EOS

333 We identified 3 characteristic areas within the Tibetan Plateau, which exhibited differing  
334 primary drivers of the changes in EOS; south western, central and eastern.

335 In the relatively arid areas of the southwestern Tibetan Plateau, the EOS exhibited a  
336 significant positive partial correlation with pre-season cumulative precipitation but a  
337 significant negative correlation with pre-season maximum temperature (Figure 3a, c).  
338 Plant available water is important for the growth of vegetation and it is usually not  
339 sufficient in arid or semi-arid regions due to high soil salinity and low water content  
340 (Wang et al., 2022). Our results indicated that, in the southwestern Tibetan Plateau,  
341 higher pre-season precipitation significantly delayed the EOS although this was

342 constrained by pre-season maximum temperatures tending to significantly advance the  
343 EOS. As the climate in this southwestern region is dry and the pre-season soil moisture is  
344 low (Figure 4), an increase in pre-season precipitation can alleviate water stress,  
345 enhancing water use efficiency (Liu et al., 2016; Munné-Bosch et al., 2004) and  
346 delaying the EOS. At the same time, an increase in maximum temperature would  
347 increase hydrological losses through evaporation and reduce the amount of available  
348 water (Kelsey et al., 2021; Shen et al., 2016), inhibiting the growth of marsh vegetation  
349 (Shen, Liu, et al., 2021). These dynamics fit well with our results, indicating that the  
350 EOS was primarily affected by precipitation in the southwestern arid regions of the  
351 study area. For the first time, our results indicate that, even in marsh ecosystems with  
352 their relatively high water contents, available water may be insufficient for vegetation  
353 growth in the drier regions of the Tibetan Plateau.

354 In the central Tibetan Plateau, a higher pre-season temperature delayed the EOS,  
355 while increased pre-season precipitation advanced it (Figure 3). In the humid and cold  
356 areas of the central Tibetan Plateau, soil moisture and temperature are higher and lower,  
357 respectively, than those in the southwestern region (Cong et al., 2017) (Figure 4). In  
358 light of these conditions, our results indicate that water was not the key factor affecting  
359 the growth of marsh vegetation in the central plateau, although temperature remained a  
360 limiting factor.

361 An increase in maximum temperature can decelerate the process of chlorophyll  
362 degradation (Shi et al., 2017) and retard the progression of leaf senescence (Estiarte et

363 al., 2017). In addition, high pre-season nighttime temperatures reduce the occurrence of  
364 frost damage (Shen, Liu, et al., 2022). By calculating the number of the frost days, we  
365 confirmed that warming pre-season nighttime temperatures had the most notable  
366 negative effect on the frost days in the central Tibetan Plateau, the coldest region of the  
367 study area (Figure S2). This could account for the role of increasing minimum  
368 temperature in delaying the EOS in the central Tibetan Plateau. In contrast, increased  
369 pre-season precipitation could retard the growth of marsh vegetation due to the  
370 accompanying cooling effect, which would advance the EOS in the already cold and  
371 humid areas of the central Tibetan Plateau.

372 In the low altitude humid regions in the east and high-altitude cold permafrost  
373 regions in the west, the EOS showed a significant positive correlation with pre-season  
374 minimum temperature (Figure 3), indicating that an increase in this parameter delayed  
375 the EOS in the marshes distributed in these regions of the Tibetan Plateau. However, the  
376 mechanisms through which minimum temperature affects the EOS may differ between  
377 these two areas. On one hand, increased nighttime temperatures cause a greater loss of  
378 organic matter due to enhanced respiration, but on the other hand it can also stimulate  
379 accumulation of more organic matter via the overcompensation effect (Shen, Liu, et al.,  
380 2021, 2022), a phenomenon through which the vegetation recovers and exceeds its  
381 original state by promoting photosynthesis the day after the enhanced respiration (Peng  
382 et al., 2013). It has been reported that the occurrence of this effect is favored by the  
383 presence of sufficient water and nutrients (Peng et al., 2013; Shen, Liu, et al., 2022).

384 In cold high-altitude regions, the physiological processes causing vegetation  
385 senescence are typically determined by low temperatures during cold nights (Tang et al.,  
386 2016). In the high-altitude cold permafrost regions of the western Tibetan Plateau,  
387 nighttime minimum temperature is generally low (Nan et al., 2005), and an increase in  
388 pre-season minimum temperature would delay the EOS by alleviating frost damage and  
389 retarding vegetation senescence (Cong et al., 2017). In contrast, in the low altitude area  
390 of the eastern Tibetan Plateau, the climate is relatively warm and humid (Figure 4) and  
391 marsh vegetation has access to sufficient water (Shen, Liu, et al., 2022). Therefore,  
392 although organic matter may be depleted through the respiration of marsh vegetation  
393 due to nighttime warming, increased temperatures can also promote photosynthesis,  
394 leading to accumulation of more organic matter the following day via the over  
395 compensation effect (Belsky et al., 1986; Shen, Liu, et al., 2021, 2022). This would  
396 contribute to delaying the EOS in the eastern region as a consequence of the increased  
397 pre-season minimum temperatures.

398 By building a multi-variable regression for each pixel, we showed spatially which  
399 pre-season variable is the most important for affecting the EOS. The results confirmed  
400 that pre-season cumulative precipitation and minimum temperature played a crucial role  
401 in the relatively arid southwestern and humid eastern Tibetan Plateau, respectively  
402 (Figure S3). By comparing the partial correlation coefficients between EOS and climatic  
403 factors in different regions, we confirmed that as annual mean temperature increased,  
404 the delaying effects of higher pre-season maximum and minimum temperatures on the

405 EOS gradually weakened, while the delaying effect of increased pre-season precipitation  
406 became gradually stronger (Figure 5). Based on our results, we propose that the effects  
407 of climate variations on the EOS differ depending on the hydrological constraints on  
408 soil moisture in the marshes within the Tibetan Plateau. As such, we further compared  
409 the partial correlations between EOS and climatic factors for pre-season soil moisture  
410 gradients of  $0.03 \text{ m}^3/\text{m}^3$ . The results showed that as soil moisture increased, the delaying  
411 effect of increased pre-season precipitation on the EOS gradually weakened (Figure 3),  
412 while the delaying effects of higher pre-season maximum and minimum temperatures  
413 became gradually stronger (Figure 3). This finding supports the proposal that increased  
414 precipitation and warming temperatures significantly delayed the EOS for marsh  
415 vegetation in the arid southwestern Tibetan Plateau and the humid central and eastern  
416 areas, respectively. In contrast, increasing daytime temperatures and precipitation  
417 advanced the EOS in the arid southwestern and humid central areas due to the reduced  
418 soil moisture and cooling effect, respectively (Figure 3).

419

#### 420 4.4 Attribution of temporal changes in the EOS

421 To further explain the temporal and spatial variations in the EOS, we calculated the  
422 rates at which precipitation and maximum and minimum temperatures varied on the  
423 plateau from 2001 to 2020 (Figure 6 and Table 1). The pre-season cumulative  
424 precipitation and minimum temperature exhibited increasing trends ( $0.52 \text{ mm/a}$  and  
425  $0.05 \text{ }^\circ\text{C/a}$ , respectively), and the increase in the minimum temperature was significant

426 ( $P < 0.05$ ). Because the EOS showed a significant positive relationship with preseason  
 427 minimum temperature, the increase in this parameter may partly account for the delayed  
 428 EOS on the Tibetan Plateau (Figure 1 and Table 1).

429 Table 1 Temporal trends of preseason and seasonal precipitation (mm/a), maximum  
 430 temperature ( $^{\circ}\text{C}/\text{a}$ ), and minimum temperature ( $^{\circ}\text{C}/\text{a}$ ) in marshes of the Tibetan Plateau  
 431 from 2001 to 2020.

	Precipitation	Maximum temperature	Minimum temperature
Preseason	0.52*	-0.02	0.05*
Spring	0.22	0.01	0.05**
Summer	0.31	0.05*	0.06*
Autumn	0.14	0.05	0.08**
Winter	0.79	-0.03	0.03

432 \*\* $P < 0.01$ ; \* $P < 0.05$ .

433 In the high-altitude arid area of the southwestern Tibetan Plateau, the EOS was  
 434 positively correlated with preseason cumulative precipitation (Figure 3). As preseason  
 435 cumulative precipitation showed significant increasing trends in the high-altitude arid  
 436 area of the southwestern Tibetan Plateau (Figure 6), the increase in preseason  
 437 cumulative precipitation may partly account for the delayed EOS in this region (Figure  
 438 1). In the low altitude humid areas in the east and high-altitude cold permafrost areas in  
 439 the west, the EOS was positively correlated with preseason minimum temperature

440 (Figure 3). Therefore, we deduce that the extremely significant increases of pre-season  
441 minimum temperature may contribute to the delayed EOS in these regions (Figures 1  
442 and 6). In the northeastern area of the plateau, the EOS appeared to occur earlier  
443 throughout the study period (Figure 1), possibly due to the rise in pre-season minimum  
444 temperature (Figures 3 and 6). Previous studies have shown that the Tibetan Plateau will  
445 become warmer and wetter in the future (Shen, Liu, et al., 2022), therefore the EOS of  
446 marsh may continue to be delayed to some extent in the future, especially in the  
447 southwestern Tibetan Plateau.

448

## 449 **5 Conclusions**

450 Our study reveals several crucial findings regarding the end of the growing season (EOS)  
451 in marsh vegetation across the Tibetan Plateau. Firstly, we observed a significant delay  
452 in the EOS by 4.10 days/decade during the study period. Secondly, while average  
453 pre-season cumulative precipitation did not notably impact the regionally averaged EOS,  
454 warmer pre-season temperatures led to a significant delay in the average EOS of marsh  
455 vegetation. Notably, the delaying effect of higher nighttime temperatures on the  
456 regionally averaged EOS was more pronounced than that of daytime temperatures. This  
457 asymmetric response to diurnal temperature variations can be attributed to the  
458 widespread delaying effect of nighttime warming and the spatially diverse relationship  
459 between EOS and daytime temperature, influenced by water conditions. Furthermore,  
460 our evidence indicates that hydrological factors influencing soil water content play a

461 regulatory role in the impact of climate change on the EOS. As soil moisture decreased,  
462 the delaying effect of increasing pre-season maximum temperatures gradually weakened  
463 and even reversed, while the delaying effect of increased pre-season precipitation was  
464 strengthened. In the humid, cold regions of the central Tibetan Plateau, higher pre-season  
465 maximum temperatures significantly delayed the EOS, whereas increased precipitation  
466 advanced it, potentially due to a cooling effect. In the low altitude, humid regions in the  
467 east, higher minimum temperatures delayed the EOS, possibly due to an  
468 overcompensation effect. In the arid southwestern area, increased precipitation directly  
469 and significantly delayed the EOS, whereas higher daytime temperatures advanced it,  
470 likely due to limited water availability. These findings suggest that the EOS in these  
471 regions is constrained by water conditions, even within marsh ecosystems. As the marsh  
472 in the Tibetan Plateau is a typical alpine freshwater marsh, our findings can provide  
473 some implications for other studies of alpine freshwater marsh. Overall, this study  
474 highlights the asymmetric influences of daytime and nighttime temperatures on the EOS  
475 of marsh vegetation, particularly in the context of global diurnal asymmetric warming  
476 (stronger warming during nighttime than during daytime). It underscores the importance  
477 of considering water conditions in EOS simulations conducted by terrestrial ecosystem  
478 models in cold and dry regions worldwide.

479

#### 480 **Author contributions**

481 **Xiangjin Shen:** Conceptualization; Data Curation; Formal Analysis; Funding



482 Acquisition; Investigation; Methodology; Resources; Validation; Visualization; Writing  
483 – Original Draft Preparation; Writing – Review & Editing. **Miaogen Shen:**  
484 Conceptualization; Data Curation; Formal Analysis; Investigation; Methodology;  
485 Resources; Validation; Visualization; Writing – Original Draft Preparation; Writing –  
486 Review & Editing. **Chaoyang Wu:** Data Curation; Formal Analysis; Methodology;  
487 Resources; Visualization; Writing – Original Draft Preparation; Writing – Review &  
488 Editing. **Josep Peñuelas:** Formal Analysis; Funding Acquisition; Writing – Review &  
489 Editing. **Philippe Ciais:** Formal Analysis; Writing – Review & Editing. **Jiaqi Zhang:**  
490 Data Curation; Formal Analysis; Investigation; Validation; Visualization; Writing –  
491 Original Draft Preparation; Writing – Review & Editing. **Chris Freeman:** Formal  
492 Analysis; Writing – Review & Editing. **Paul I. Palmer:** Formal Analysis; Writing –  
493 Review & Editing. **Binhui Liu:** Methodology; Writing – Review & Editing. **Mark**  
494 **Henderson:** Formal Analysis; Writing – Review & Editing. **Zhaoliang Song:** Writing  
495 – Review & Editing. **Shaobo Sun:** Writing – Review & Editing. **Xianguo Lu:**  
496 Conceptualization; Formal Analysis; Methodology; Resources; Writing – Review &  
497 Editing. **Ming Jiang:** Conceptualization; Formal Analysis; Funding Acquisition;  
498 Methodology; Project Administration; Resources; Supervision; Writing – Review &  
499 Editing.

500

## 501 **Acknowledgements**

502 We gratefully acknowledge the National Natural Science Foundation of China

503 (42230516, 41971065), Key Research Program of Frontier Sciences, Chinese Academy  
504 of Sciences (ZDBS-LY-7019), Youth Innovation Promotion Association, Chinese  
505 Academy of Sciences (2019235), Natural Science Foundation of Jilin Province  
506 (20210101104JC), and the Spanish Government grant TED2021-132627 B-I00, funded  
507 by MCIN, AEI/10.13039/ 501100011033 European Union Next Generation EU/PRTR.

508

#### 509 **Conflict of interest statement**

510 The authors declare no conflict of interest.

511

#### 512 **Data availability statement**

513 The NDVI dataset (MOD13Q1) was provided by the Earth Science Data Systems of the  
514 National Aeronautics and Space Administration  
515 (<https://ladsweb.modaps.eosdis.nasa.gov>). The distribution dataset of marshes was  
516 obtained from the wetland distribution datasets for China (30 m wetland distribution  
517 thematic data in China) (<http://www.geodata.cn>). The soil moisture data (1 km daily soil  
518 moisture dataset over China) were obtained from the National Tibetan Plateau Scientific  
519 Data Center (<https://data.tpsc.ac.cn/en/data/49b22de9-5d85-44f2-a7d5-a1ccd17086d2/>).  
520 Metadata that support the findings of this study are available from Zenodo  
521 at <https://doi.org/10.5281/zenodo.10258355>.

522

#### 523 **References**

524 Bao, G., Tuya, A., Bayarsaikhan, S., Dorjsuren, A., Mandakh, U., Bao, Y., Li, C., &  
525 Vanchindorj, B. (2020). Variations and climate constraints of terrestrial net primary  
526 productivity over Mongolia. *Quaternary International*, 537, 112-125.  
527 <https://doi.org/10.1016/j.quaint.2019.06.017>

528 Belsky, A. J. (1986). Does herbivory benefit plants? A review of the evidence. *The*  
529 *American Naturalist*, 127, 870-892. <https://doi.org/10.1086/284531>

530 Che, M., Chen, B., Innes, J. L., Wang, G., Dou, X., Zhou, T., Zhang, H., Yan, J., Xu, G.,  
531 & Zhao, H. (2014). Spatial and temporal variations in the end date of the  
532 vegetation growing season throughout the Qinghai–Tibetan Plateau from 1982 to  
533 2011. *Agricultural and Forest Meteorology*, 189, 81-90.  
534 <https://doi.org/10.1016/j.agrformet.2014.01.004>

535 Chen, X. (2017). Plant phenology of natural landscape dynamics. In *Spatiotemporal*  
536 *processes of plant phenology*. Springer, Berlin, Heidelberg.

537 Chen, X., An, S., Inouye, D. W., & Schwartz, M. D. (2015). Temperature and snowfall  
538 trigger alpine vegetation green-up on the world's roof. *Global Change Biology*, 21,  
539 3635-3646. <https://doi.org/10.1111/gcb.12954>

540 Cheng, M., Jin, J., & Jiang, H. (2021). Strong impacts of autumn phenology on  
541 grassland ecosystem water use efficiency on the Tibetan Plateau. *Ecological*  
542 *Indicators*, 126, 107682. <https://doi.org/10.1016/j.ecolind.2021.107682>

543 Coleman, D. J., Schuerch, M., Temmerman, S., Guntenspergen, G., Smith, C. G., &  
544 Kirwan, M. L. (2022). Reconciling models and measurements of marsh

545 vulnerability to sea level rise. *Limnology and Oceanography Letters*, 7, 140-149.  
546 <https://doi.org/10.1002/lol2.10230>

547 Cong, N., Shen, M., & Piao, S. (2017). Spatial variations in responses of vegetation  
548 autumn phenology to climate change on the Tibetan Plateau. *Journal of Plant  
549 Ecology*, 10, 744-752. <https://doi.org/10.1093/jpe/rtw084>

550 Cong, N., Wang, T., Nan, H., Ma, Y., Wang, X., Myneni, R. B., & Piao, S. (2013).  
551 Changes in satellite-derived spring vegetation green-up date and its linkage to  
552 climate in China from 1982 to 2010: a multimethod analysis. *Global Change  
553 Biology*, 19, 881-891. <https://doi.org/10.1111/gcb.12077>

554 Dong, M., Jiang, Y., Zheng, C., & Zhang, D. (2012). Trends in the thermal growing  
555 season throughout the Tibetan Plateau during 1960-2009. *Agricultural and Forest  
556 Meteorology*, 166, 201-206. <https://doi.org/10.1016/j.agrformet.2012.07.013>

557 Dorji, T., Totland, Ø., Moe, S. R., Hopping, K. A., Pan, J., & Klein, J. A. (2013). Plant  
558 functional traits mediate reproductive phenology and success in response to  
559 experimental warming and snow addition in Tibet. *Global Change Biology*, 19,  
560 459-472. <https://doi.org/10.1111/gcb.12059>

561 Estiarte, M., & Peñuelas, J. (2015). Alteration of the phenology of leaf senescence and  
562 fall in winter deciduous species by climate change: effects on nutrient proficiency.  
563 *Global Change Biology*, 21, 1005-1017. <https://doi.org/10.1111/gcb.12804>

564 Fu, Y. H., Piao, S., Delpierre, N., Hao, F., Hänninen, H., Liu, Y., Sun, W., Janssens, I. A.,  
565 & Campioli, M. (2018). Larger temperature response of autumn leaf senescence

566 than spring leaf - out phenology. *Global Change Biology*, 24, 2159-2168.  
567 <https://doi.org/10.1111/gcb.14021>

568 Fu, Y. H., Piao, S., Op de Beeck, M., Cong, N., Zhao, H., Zhang, Y., Menzel, A., &  
569 Janssens, I. A. (2014). Recent spring phenology shifts in western Central Europe  
570 based on multiscale observations. *Global Ecology and Biogeography*, 23,  
571 1255-1263. <https://doi.org/10.1111/geb.12210>

572 Jeong, S. J., HO, C. H., GIM, H. J., & Brown, M. E. (2011). Phenology shifts at start vs.  
573 end of growing season in temperate vegetation over the Northern Hemisphere for  
574 the period 1982–2008. *Global Change Biology*, 17, 2385-2399.  
575 <https://doi.org/10.1111/j.1365-2486.2011.02397.x>

576 Ganguly, S., Friedl, M. A., Tan, B., Zhang, X., & Verma, M. (2010). Land surface  
577 phenology from MODIS: Characterization of the Collection 5 global land cover  
578 dynamics product. *Remote Sensing of Environment*, 114, 1805-1816.  
579 <https://doi.org/10.1016/j.rse.2010.04.005>

580 Ganjurjav, H., Gornish, E. S., Hu, G., Schwartz, M. W., Wan, Y., Li, Y., & Gao, Q.  
581 (2020). Warming and precipitation addition interact to affect plant spring  
582 phenology in alpine meadows on the central Qinghai-Tibetan Plateau. *Agricultural  
583 and Forest Meteorology*, 287, 107943.  
584 <https://doi.org/10.1016/j.agrformet.2020.107943>

585 Gao, Y. C., & Liu, M. (2013). Evaluation of high-resolution satellite precipitation  
586 products using rain gauge observations over the Tibetan Plateau. *Hydrology and*

587 *Earth System Sciences*, 17, 837-849. <https://doi.org/10.5194/hess-17-837-2013>

588 Garonna, I., De Jong, R., De Wit, A. J., Mùcher, C. A., Schmid, B., & Schaepman, M. E.  
589 (2014). Strong contribution of autumn phenology to changes in satellite - derived  
590 growing season length estimates across Europe (1982-2011). *Global Change*  
591 *Biology*, 20, 3457-3470. <https://doi.org/10.1111/gcb.12625>

592 Ge, Q., Wang, H., Rutishauser, T., & Dai, J. (2015). Phenological response to climate  
593 change in China: a meta-analysis. *Global Change Biology*, 21, 265-274.  
594 <https://doi.org/10.1111/gcb.12648>

595 Kafaki, S. B., Mataji, A., & Hashemi, S. A. (2009). Monitoring growing season length  
596 of deciduous broad leaf forest derived from satellite data in Iran. *American Journal*  
597 *of Environmental Sciences*, 5, 647-652. <http://doi.org/10.3844/ajessp.2009.647.652>

598 Kelsey, K. C., Pedersen, S. H., Leffler, A. J., Sexton, J. O., Feng, M., & Welker, J. M.  
599 (2021). Winter snow and spring temperature have differential effects on vegetation  
600 phenology and productivity across Arctic plant communities. *Global Change*  
601 *Biology*, 27, 1572-1586. <https://doi.org/10.1111/gcb.15505>

602 Keppeler, F. W., Olin, J. A., López - Duarte, P. C., Polito, M. J., Hooper - Bùì, L. M.,  
603 Taylor, S. S., Rabalais, N. N., Fodrie F. J., Roberts, B. J., Turner, R. R., Matin, C.  
604 W., & Jensen, O. P. (2021). Body size, trophic position, and the coupling of  
605 different energy pathways across a saltmarsh landscape. *Limnology and*  
606 *Oceanography Letters*, 6, 360-368. <https://doi.org/10.1002/lol2.10212>

607 Lee, R., Yu, F., Price, K. P., Ellis, J., & Piao, S. (2002). Evaluating vegetation

608 phenological patterns in Inner Mongolia using NDVI time-series analysis.  
609 *International Journal of Remote Sensing*, 23, 2505-2512.  
610 <https://doi.org/10.1080/01431160110106087>

611 Li, Q., Shi, G., Shangguan, W., Nourani, V., Li, J., Li, L., Huang, F., Zhang, Y., Wang,  
612 C., Wang, D., Qiu, J., Lu, X., & Dai, Y. (2022). A 1 km daily soil moisture dataset  
613 over China using in situ measurement and machine learning, *Earth System Science*  
614 *Data*, 14, 5267–5286. <https://doi.org/10.5194/essd-14-5267-2022>

615 Li, Z., Lai, Q., Bao, Y., Liu, X., Na, Q., Li, Y. (2023). Variations in Phenology  
616 Identification Strategies across the Mongolian Plateau Using Multiple Data  
617 Sources and Methods. *Remote Sensing*, 15, 4237.  
618 <https://doi.org/10.3390/rs15174237>

619 Lin, S., Wang, G., Hu, Z., Huang, K., Sun, J., & Sun, X. (2020). Spatiotemporal  
620 variability and driving factors of Tibetan Plateau water use efficiency. *Journal of*  
621 *Geophysical Research: Atmospheres*, 125, e2020JD032642.  
622 <https://doi.org/10.1029/2020JD032642>

623 Liu, Q., Fu, Y. H., Zeng, Z., Huang, M., Li, X., & Piao, S. (2016). Temperature,  
624 precipitation, and insolation effects on autumn vegetation phenology in temperate  
625 China. *Global Change Biology*, 22, 644-655. <https://doi.org/10.1111/gcb.13081>

626 Liu, X., Chen, Y., Li, Z., Li, Y., Zhang, Q., & Zan, M. (2021). Driving Forces of the  
627 Changes in Vegetation Phenology in the Qinghai–Tibet Plateau. *Remote Sensing*,  
628 13, 4952. <https://doi.org/10.3390/rs13234952>

629 Liu, Y., Shen, X., Zhang, J., Wang, Y., Wu, L., Ma, R., Lu, X., & Jiang, M. (2023).  
630 Spatiotemporal variation in vegetation phenology and its response to climate  
631 change in marshes of Sanjiang Plain, China. *Ecology and Evolution*, *13*, e9755.  
632 <https://doi.org/10.1002/ece3.9755>

633 Ma, R., Shen, X., Zhang, J., Xia, C., Liu, Y., Wu, L., Wang, Y., Jiang, M., & Lu, X.  
634 (2022). Variation of vegetation autumn phenology and its climatic drivers in  
635 temperate grasslands of China. *International Journal of Applied Earth Observation*  
636 *and Geoinformation*, *114*, 103064. <https://doi.org/10.1016/j.jag.2022.103064>

637 Mao, D., Wang, Z., Du, B., Li, L., Tian, Y., Jia, M., Zeng, Y., Song, K., Jiang, M., &  
638 Wang, Y. (2020). National wetland mapping in China: A new product resulting  
639 from object-based and hierarchical classification of Landsat 8 OLI images. *ISPRS*  
640 *Journal of Photogrammetry and Remote Sensing*, *164*, 11-25.  
641 <https://doi.org/10.1016/j.isprsjprs.2020.03.020>

642 Molino, G. D., Carr, J. A., Ganju, N. K., & Kirwan, M. L. (2022). Variability in marsh  
643 migration potential determined by topographic rather than anthropogenic  
644 constraints in the Chesapeake Bay region. *Limnology and Oceanography Letters*, *7*,  
645 321-331. <https://doi.org/10.1002/lol2.10262>

646 Munné-Bosch, S., & Alegre, L. (2004). Die and let live: leaf senescence contributes to  
647 plant survival under drought stress. *Functional Plant Biology*, *31*, 203-216.  
648 <https://doi.org/10.1071/FP03236>

649 Nan, Z., Li, S., & Cheng, G. (2005). Prediction of permafrost distribution on the



650 Qinghai-Tibet Plateau in the next 50 and 100 years. *Science in China Series D:*  
651 *Earth Sciences*, 48, 797-804. <https://doi.org/10.1360/03yd0258>

652 Niu, L., Guo, Y., Li, Y., Wang, C., Hu, Q., Fan, L., Wang, L., & Yang, N. (2021).  
653 Degradation of river ecological quality in Tibet plateau with overgrazing: A  
654 quantitative assessment using biotic integrity index improved by random  
655 forest. *Ecological Indicators*, 120, 106948.  
656 <https://doi.org/10.1016/j.ecolind.2020.106948>

657 Peng, S., Piao, S., Ciais, P., Myneni, R. B., Chen, A., Chevallier, F., Dolman, A. J.,  
658 Janssens, I. A., Penuelas, J., Zhang, G., Vicca, S., Wan, S., Wang, S., & Zeng, H.  
659 (2013). Asymmetric effects of daytime and night-time warming on Northern  
660 Hemisphere vegetation. *Nature*, 501, 88-92. <https://doi.org/10.1038/nature12434>

661 Peñuelas, J., Filella, I. (2001). Responses to a warming world. *Science*, 294(5543):  
662 793-795. <https://doi.org/10.1126/science.10668>.

663 Piao, S., Ciais, P., Friedlingstein, P., Peylin, P., Reichstein, M., Luysaert, S., Margolis,  
664 H., Fang, J., Barr, A., Chen, A., Grelle, A., Hollinger, D. Y., Laurila, T., Lindroth,  
665 A., Richardson, A. D., & Vesala, T. (2008). Net carbon dioxide losses of northern  
666 ecosystems in response to autumn warming. *Nature*, 451, 49-52.  
667 <https://doi.org/10.1038/nature06444>

668 Piao, S., Cui, M., Chen, A., Wang, X., Ciais, P., Liu, J., & Tang, Y. (2011). Altitude and  
669 temperature dependence of change in the spring vegetation green-up date from  
670 1982 to 2006 in the Qinghai-Xizang Plateau. *Agricultural and Forest Meteorology*,

671 151, 1599-1608. <https://doi.org/10.1016/j.agrformet.2011.06.016>

672 Piao, S., Fang, J., Zhou, L., Ciais, P., & Zhu, B. (2006). Variations in satellite-derived  
673 phenology in China's temperate vegetation. *Global Change Biology*, 12, 672-685.  
674 <https://doi.org/10.1111/j.1365-2486.2006.01123.x>

675 Piao, S., Friedlingstein, P., Ciais, P., Viovy, N., & Demarty, J. (2007). Growing season  
676 extension and its impact on terrestrial carbon cycle in the Northern Hemisphere  
677 over the past 2 decades. *Global Biogeochemical Cycles*, 21.  
678 <https://doi.org/10.1029/2006GB002888>

679 Piao, S., Liu, Q., Chen, A., Janssens, I. A., Fu, Y., Dai, J., Liu, L., Lian, X., Shen, M., &  
680 Zhu, X. (2019). Plant phenology and global climate change: Current progresses  
681 and challenges. *Global Change Biology*, 25, 1922-1940.  
682 <https://doi.org/10.1111/gcb.14619>

683 Piao, S., Tan, J., Chen, A., Fu, Y. H., Ciais, P., Liu, Q., Janssens, I. A., Vicca, S., Zeng, Z.,  
684 Jeong, S., Li, Y., R. B., Myneni, Peng, S., Shen, M., Peñuelas, J. (2015). Leaf onset  
685 in the northern hemisphere triggered by daytime temperature. *Nature*  
686 *Communications*, 6, 6911. <https://doi.org/10.1038/ncomms7911>

687 Qin, G., Adu, B., Li, C., & Wu, J. (2022). Diverse Responses of Phenology in  
688 Multi-Grassland to Environmental Factors on Qinghai–Tibetan Plateau in China.  
689 *Theoretical and Applied Climatology*, 148, 931-942.  
690 <https://doi.org/10.1007/s00704-022-03963-3>

691 Reed, B. C., Brown, J. F., Vanderzee, D., Loveland, T. S., Merchant, J. W., & Ohlen, D.

692 O. (1994). Measuring phenological variability from satellite imagery. *Journal of*  
693 *Vegetation Science*, 5, 703-714. <https://doi.org/10.2307/3235884>

694 Rice, K. E., Montgomery, R. A., Stefanski, A., Rich, R. L., & Reich, P. B. (2018).  
695 Experimental warming advances phenology of groundlayer plants at the boreal -  
696 temperate forest ecotone. *American Journal of Botany*, 105, 851-861.  
697 <https://doi.org/10.1002/ajb2.1091>

698 Richardson, A. D., Keenan, T. F., Migliavacca, M., Ryu, Y., Sonnentag, O., & Toomey,  
699 M. (2013). Climate change, phenology, and phenological control of vegetation  
700 feedbacks to the climate system. *Agricultural and Forest Meteorology*, 169,  
701 156-173. <https://doi.org/10.1016/j.agrformet.2012.09.012>

702 Shen, M., Piao, S., Chen, X., An, S., Fu, Y. H., Wang, S., Cong, N., & Janssens, I. A.  
703 (2016). Strong impacts of daily minimum temperature on the green-up date and  
704 summer greenness of the Tibetan Plateau. *Global Change Biology*, 22, 3057-3066.  
705 <https://doi.org/10.1111/gcb.13301>

706 Shen, M., Piao, S., Cong, N., Zhang, G., & Janssens, I. A. (2015). Precipitation impacts  
707 on vegetation spring phenology on the Tibetan Plateau. *Global Change Biology*, 21,  
708 3647-3656. <https://doi.org/10.1111/gcb.12961>

709 Shen, M., Piao, S., Dorji, T., Liu, Q., Cong, N., Chen, X., An, S., Wang, S., Wang, T., &  
710 Zhang, G. (2015). Plant phenological responses to climate change on the Tibetan  
711 Plateau: research status and challenges. *National Science Review*, 2, 454-467.  
712 <https://doi.org/10.1093/nsr/nwv058>

713 Shen, M., Tang, Y., Chen, J., Zhu, X., & Zheng, Y. (2011). Influences of temperature  
714 and precipitation before the growing season on spring phenology in grasslands of  
715 the central and eastern Qinghai-Tibetan Plateau. *Agricultural and Forest  
716 Meteorology*, *151*, 1711-1722. <https://doi.org/10.1016/j.agrformet.2011.07.003>

717 Shen, M., Wang, S., Jiang, N., Sun, J., Cao, R., Ling, X., Fang, B., Zhang, L., Zhang, L.,  
718 Xu, X., Lv, W., Li, B., Sun, Q., Meng, F., Jiang, Y., Dorji, T., Fu, Y., Iier, A.,  
719 Vitasse, Y., Steltzer, H., Ji, Z., Zhao, W., Piao, S., & Fu, B. (2022). Plant phenology  
720 changes and drivers on the Qinghai–Tibetan Plateau. *Nature Reviews Earth &  
721 Environment*, *3*, 633-651. <https://doi.org/10.1038/s43017-022-00317-5>

722 Shen, M., Zhang, G., Cong, N., Wang, S., Kong, W., & Piao, S. (2014). Increasing  
723 altitudinal gradient of spring vegetation phenology during the last decade on the  
724 Qinghai–Tibetan Plateau. *Agricultural and Forest Meteorology*, *189*, 71-80.  
725 <https://doi.org/10.1016/j.agrformet.2014.01.003>

726 Shen, X., Jiang, M., & Lu, X. (2023). Diverse impacts of day and night temperature on  
727 spring phenology in freshwater marshes of the Tibetan Plateau. *Limnology and  
728 Oceanography Letters*, *8*, 323-329. <https://doi.org/10.1002/lol2.10285>

729 Shen, X., Jiang, M., Lu, X., Liu, X., Liu, B., Zhang, J., Wang, X., Tong, S., Lei, G.,  
730 Wang, S., Tong, C., Fan, H., Tian, K., Wang, X., Hu, Y., Xie, Y., Ma, M., Zhang, S.,  
731 Cao, C., & Wang, Z. (2021). Aboveground biomass and its spatial distribution  
732 pattern of herbaceous marsh vegetation in China. *Science China Earth Sciences*, *64*,  
733 1115-1125. <https://doi.org/10.1007/s11430-020-9778-7>

- 734 Shen, X., Liu, B., Henderson, M., Wang, L., Wu, Z., Wu, H., Jiang, M., & Lu, X. (2018).  
735 Asymmetric effects of daytime and nighttime warming on spring phenology in the  
736 temperate grasslands of China. *Agricultural and Forest Meteorology*, 259, 240-249.  
737 <https://doi.org/10.1016/j.agrformet.2018.05.006>
- 738 Shen, X., Liu, B., Jiang, M., Wang, Y., Wang, L., Zhang, J., & Lu, X. (2021).  
739 Spatiotemporal change of marsh vegetation and its response to climate change in  
740 China from 2000 to 2019. *Journal of Geophysical Research: Biogeosciences*, 126,  
741 e2020JG006154. <https://doi.org/10.1029/2020JG006154>
- 742 Shen, X., Liu, B., Xue, Z., Jiang, M., Lu, X., & Zhang, Q. (2019). Spatiotemporal  
743 variation in vegetation spring phenology and its response to climate change in  
744 freshwater marshes of Northeast China. *Science of the Total Environment*, 666,  
745 1169-1177. <https://doi.org/10.1016/j.scitotenv.2019.02.265>
- 746 Shen, X., Liu, Y., Zhang, J., Wang, Y., Ma, R., Liu, B., Lu, X., & Jiang, M. (2022).  
747 Asymmetric impacts of diurnal warming on vegetation carbon sequestration of  
748 marshes in the Qinghai Tibet Plateau. *Global Biogeochemical Cycles*, 36,  
749 e2022GB007396. <https://doi.org/10.1029/2022GB007396>
- 750 Shi, C., Sun, G., Zhang, H., Xiao, B., Ze, B., Zhang, N., & Wu, N. (2014). Effects of  
751 warming on chlorophyll degradation and carbohydrate accumulation of alpine  
752 herbaceous species during plant senescence on the Tibetan Plateau. *PLoS One*, 9,  
753 e107874. <https://doi.org/10.1371/journal.pone.0107874>
- 754 Su, M., Huang, X., Xu, Z., Zhu, W., & Lin, Z. (2022). A decrease in the daily maximum

755 temperature during global warming hiatus causes a delay in spring phenology in  
756 the China–DPRK–Russia cross-border area. *Remote Sensing*, *14*, 1462.  
757 <https://doi.org/10.3390/rs14061462>

758 Tang, J., Körner, C., Muraoka, H., Piao, S., Shen, M., Thackeray, S. J., & Yang, X.  
759 (2016). Emerging opportunities and challenges in phenology: a review. *Ecosphere*,  
760 *7*, e01436. <https://doi.org/10.1002/ecs2.1436>

761 Turnbull, M. H., Murthy, R., & Griffin, K. L. (2002). The relative impacts of daytime  
762 and night - time warming on photosynthetic capacity in *Populus deltoides*. *Plant*,  
763 *Cell & Environment*, *25*, 1729-1737.  
764 <https://doi.org/10.1046/j.1365-3040.2002.00947.x>

765 Wang, H., Liu, G. H., Li, Z. S., Ye, X., Wang, M., & Gong, L. (2016). Driving force and  
766 changing trends of vegetation phenology in the Loess Plateau of China from 2000  
767 to 2010. *Journal of Mountain Science*, *13*, 844-856.  
768 <https://doi.org/10.1007/s11629-015-3465-2>

769 Wang, X., Wang, T., Guo, H., Liu, D., Zhao, Y., Zhang, T., Liu, Q., Piao, S. (2018).  
770 Disentangling the mechanisms behind winter snow impact on vegetation activity in  
771 northern ecosystems. *Global Change Biology*, *24*, 1651-1662.  
772 <https://doi.org/10.1111/gcb.13930>

773 Wang, Y., Shen, X., Jiang, M., Tong, S., & Lu, X. (2021). Spatiotemporal change of  
774 aboveground biomass and its response to climate change in marshes of the Tibetan  
775 Plateau. *International Journal of Applied Earth Observation and Geoinformation*,

776 102, 102385. <https://doi.org/10.1016/j.jag.2021.102385>

777 Wang, Y., Shen, X., Jiang, M., Tong, S., & Lu, X. (2022). Daytime and nighttime  
778 temperatures exert different effects on vegetation net primary productivity of  
779 marshes in the western Songnen Plain. *Ecological Indicators*, 137, 108789.  
780 <https://doi.org/10.1016/j.ecolind.2022.108789>

781 White, M. A., de Beurs, K. M., Didan, K., Inouye, D. W., Richardson, A. D., Jensen, O.  
782 P., O'keefe, J., Zhang, G., Nemani, R. R., Van leeuwen, W. J. D., Brown, J. F.,  
783 Wit, A., Schaepman, M., Lin, X., Dettinger, M., Bailey, A. S., Kimball,  
784 J., Schwartz, M. D., Baldocchi, D. D., Iee, J., & Lauenroth, W. K. (2009).  
785 Intercomparison, interpretation, and assessment of spring phenology in North  
786 America estimated from remote sensing for 1982–2006. *Global Change*  
787 *Biology*, 15, 2335-2359. <https://doi.org/10.1111/j.1365-2486.2009.01910.x>

788 Wu, C., Peng, J., Ciais, P., Peñuelas, J., Wang, H., Beguería, S., Andrew Black, T., Jassal,  
789 R. S., Zhang, X., Yuan, W., Liang, E., Wang, X., Hua, H., Liu, R., Ju, W., Fu, Y.,  
790 & Ge, Q. (2022). Increased drought effects on the phenology of autumn leaf  
791 senescence. *Nature Climate Change*, 12, 943-949.  
792 <https://doi.org/10.1038/s41558-022-01464-9>

793 Wu, C., Wang, X., Wang, H., Ciais, P., Peñuelas, J., Myneni, R. B., Desai, A. R., Gough,  
794 C. M., Gonsamo, A., Black, A. T., Jassal, R. S., Ju, W., Yuan, W., Fu, Y., Shen, M.,  
795 Li, S., Liu, R., Chen, J., & Ge, Q. (2018). Contrasting responses of autumn-leaf  
796 senescence to daytime and night-time warming. *Nature Climate Change*, 8,

797 1092-1096. <https://doi.org/10.1038/s41558-018-0346-z>

798 Wu, X., & Liu, H. (2013). Consistent shifts in spring vegetation green-up date across  
799 temperate biomes in China, 1982-2006. *Global Change Biology*, *19*, 870-880.  
800 <https://doi.org/10.1111/gcb.12086>

801 Yang, Y., Guan, H., Shen, M., Liang, W., & Jiang, L. (2015). Changes in autumn  
802 vegetation dormancy onset date and the climate controls across temperate  
803 ecosystems in China from 1982 to 2010. *Global Change Biology*, *21*, 652-665.  
804 <https://doi.org/10.1111/gcb.12778>

805 Yang, Y., Qi, N., Zhao, J., Meng, N., Lu, Z., Wang, X., Kang, L., Li, R., Ma, J., &  
806 Zheng, H. (2021). Detecting the Turning Points of Grassland Autumn Phenology  
807 on the Qinghai-Tibetan Plateau: Spatial Heterogeneity and Controls. *Remote*  
808 *Sensing*, *13*, 4797. <https://doi.org/10.3390/rs13234797>

809 Yu, F., Price, K. P., Ellis, J., & Piao, S. (2003). Response of seasonal vegetation  
810 development to climatic variations in eastern central Asia. *Remote Sensing of*  
811 *Environment*, *87*, 42-54. [https://doi.org/10.1016/S0034-4257\(03\)00144-5](https://doi.org/10.1016/S0034-4257(03)00144-5)

812 Yu, H., Luedeling, E., & Xu, J. (2010). Winter and spring warming result in delayed  
813 spring phenology on the Tibetan Plateau. *Proceedings of the National Academy of*  
814 *Sciences*, *107*, 22151-22156. <https://doi.org/10.1073/pnas.1012490107>

815 Zhang, G., Zhang, Y., Dong, J., & Xiao, X. (2013). Green-up dates in the Tibetan  
816 Plateau have continuously advanced from 1982 to 2011. *Proceedings of the*  
817 *National Academy of Sciences*, *110*, 4309-4314.



818 <https://doi.org/10.1073/pnas.1210423110>

819 Zhang, X., Friedl, M. A., Schaaf, C. B., Strahler, A. H., Hodges, J. C., Gao, F., Reed, B.  
820 C., & Huete, A. (2003). Monitoring vegetation phenology using MODIS. *Remote*  
821 *Sensing of Environment*, 84, 471-475.  
822 [https://doi.org/10.1016/S0034-4257\(02\)00135-9](https://doi.org/10.1016/S0034-4257(02)00135-9)

823 Zhou, T., Liu, M., Sun, J., Li, Y., Shi, P., Tsunekawa, A., Zhou, H., Yi, S., & Xue, X.  
824 (2020). The patterns and mechanisms of precipitation use efficiency in alpine  
825 grasslands on the Tibetan Plateau. *Agriculture, Ecosystems & Environment*, 292,  
826 106833. <https://doi.org/10.1016/j.agee.2020.106833>

827 Zhu, W., Tian, H., Xu, X., Pan, Y., Chen, G., & Lin, W. (2012). Extension of the  
828 growing season due to delayed autumn over mid and high latitudes in North  
829 America during 1982–2006. *Global Ecology and Biogeography*, 21, 260-271.  
830 <https://doi.org/10.1111/j.1466-8238.2011.00675.x>  
831

832 **Figure legends:**

833 **FIGURE 1** Spatiotemporal change of the end of the growing season (EOS) in the  
834 marshes of the Tibetan Plateau from 2001 to 2020. (a) Distribution of marshes at  
835 different altitudes on the Tibetan Plateau. (b) Spatial patterns of long term average EOS.  
836 (c) Temporal trends in EOS. (d) Temporal variations of regionally averaged EOS. The  
837 inset histograms at the bottom of (b) and (c) describe the frequency distributions of the  
838 average EOS and EOS trend. - and + in (c) show the negative (advancing) and positive  
839 (delaying) trend, respectively; \* and \*\* indicate the trend is significant ( $P < 0.05$ ) and  
840 extremely significant ( $P < 0.01$ ), respectively. The error bar and bold black line in (d)  
841 show standard error and linear trend of the regionally averaged EOS, respectively. Map  
842 lines delineate study areas and do not necessarily depict accepted national boundaries.

843

844 **FIGURE 2** Partial correlation coefficients between pre-season climatic factors and EOS  
845 of marsh vegetation on the Tibetan Plateau. \* $P < 0.05$ ; \*\* $P < 0.01$ . Correlations lacking  
846 an asterisk are non-significant ( $P > 0.05$ ).

847

848 **FIGURE 3** Relationship between EOS and pre-season climate variables for the marshes  
849 on the Tibetan Plateau from 2001 to 2020. Spatial patterns of partial correlation  
850 coefficients between EOS and pre-season cumulative precipitation (a), maximum  
851 temperature (c), and minimum temperature (e). The changes in partial correlation  
852 coefficients between EOS and pre-season cumulative precipitation (b), maximum

853 temperature (d), and minimum temperature (f) along the spatial gradient of long-term  
854 preseason soil moisture on the Tibetan Plateau from 2001 to 2020. The inset histograms  
855 at the bottom of left figures (a, c, e) display the frequency distributions of partial  
856 correlation coefficients. - and + show the negative and positive correlation, respectively;  
857 \* and \*\* indicate the correlation is significant ( $P < 0.05$ ) and extremely significant ( $P <$   
858  $0.01$ ), respectively. The body lines in the right figures (b, d, f) indicate the linear fit for  
859 the partial correlation coefficients, and the shading represents the 95% confidence band  
860 of the fits. Map lines delineate study areas and do not necessarily depict accepted  
861 national boundaries.

862

863 FIGURE 4 Impact of climate change on marsh EOS in different regions of the marshes  
864 on the Tibetan Plateau. (a) Conceptual diagrams showing the effects of climate change  
865 on the EOS. (b) Spatial distribution of long-term average preseason soil moisture  
866 ( $\text{m}^3/\text{m}^3$ ). (c) The long-term average preseason temperature ( $^{\circ}\text{C}$ ) for marsh vegetation on  
867 the Tibetan Plateau. (d) Long-term average preseason soil moisture ( $\text{m}^3/\text{m}^3$ ) and  
868 preseason temperature ( $^{\circ}\text{C}$ ) in different regions of the Tibetan Plateau. “+” and “-”  
869 indicate that the climatic variable had a significant positive and negative effect on the  
870 EOS, respectively ( $P < 0.05$ ). “++” indicates an extremely significant positive effect ( $P$   
871  $< 0.01$ ). In the southwestern Tibetan Plateau (circled in blue), increased preseason  
872 precipitation can significantly delay the EOS, while a higher preseason maximum  
873 temperature will advance it. In contrast, in the central Tibetan Plateau (circled in red), a

874 higher pre-season maximum temperature significantly delayed the EOS, while an  
875 increased pre-season precipitation advanced it. In the eastern Tibetan Plateau (circled in  
876 green), a higher pre-season minimum temperature significantly delayed the EOS. Map  
877 lines delineate study areas and do not necessarily depict accepted national boundaries.

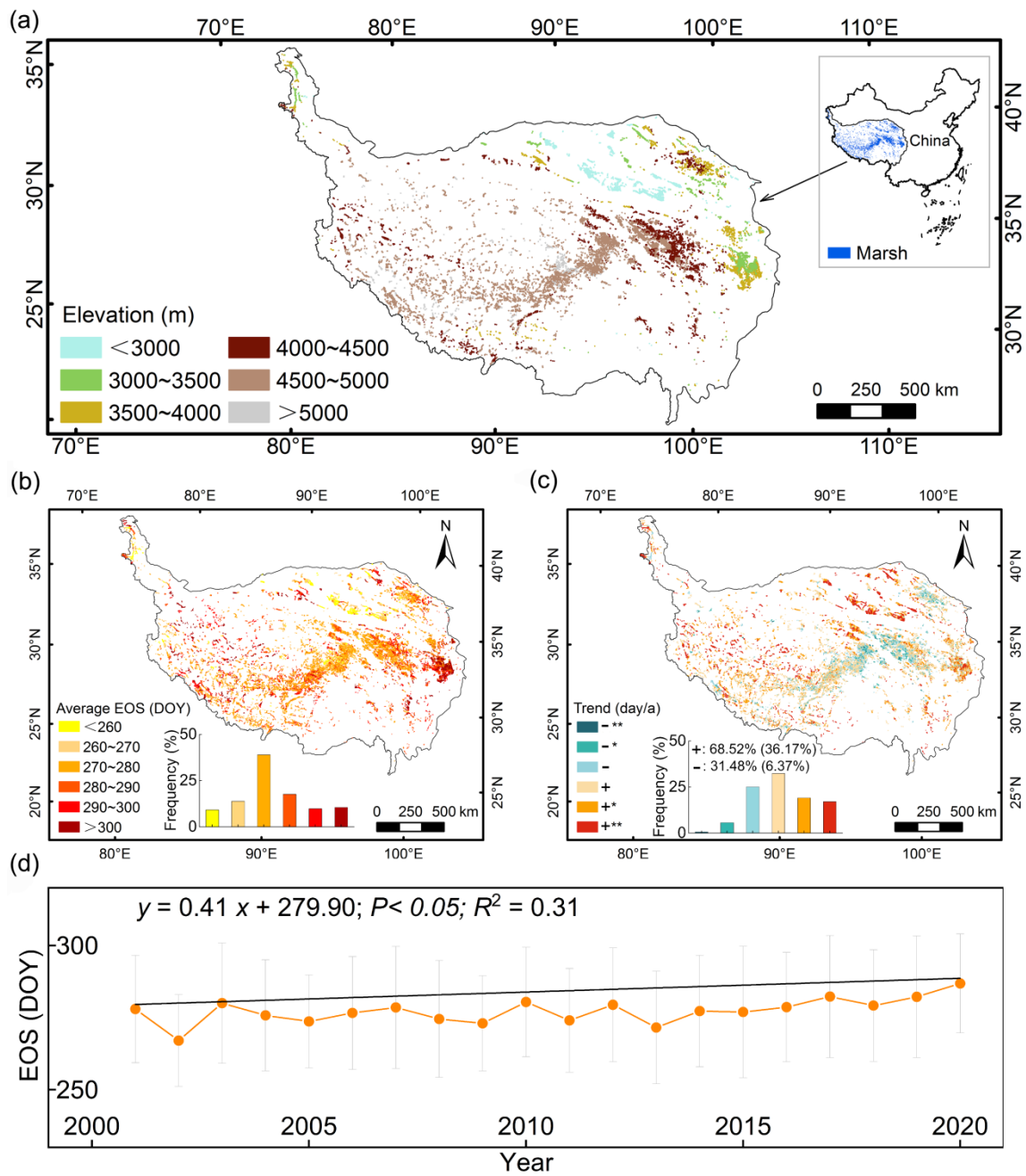
878

879 FIGURE 5 The changes in partial correlation coefficients between EOS and pre-season  
880 cumulative precipitation, maximum temperature, and minimum temperature along the  
881 spatial gradient of 1 °C for long-term annual mean temperature on the Tibetan Plateau  
882 from 2001 to 2020. The body lines in the figures indicate the linear fit for the partial  
883 correlation coefficients, and the shading represents the 95% confidence band of the fits.

884

885 FIGURE 6 Pre-season climate change in the marshes of the Tibetan Plateau. Spatial  
886 patterns of temporal trends in pre-season cumulative precipitation (a), maximum  
887 temperature (b), and minimum temperature (c) in the marshes of the Tibetan Plateau  
888 from 2001 to 2020. The inset histograms at the bottom of figures display the frequency  
889 distributions of the trends. - and + show the negative and positive trend, respectively; \*  
890 and \*\* indicate the variation trend is significant ( $P < 0.05$ ) and extremely significant ( $P$   
891  $< 0.01$ ), respectively. Map lines delineate study areas and do not necessarily depict  
892 accepted national boundaries.

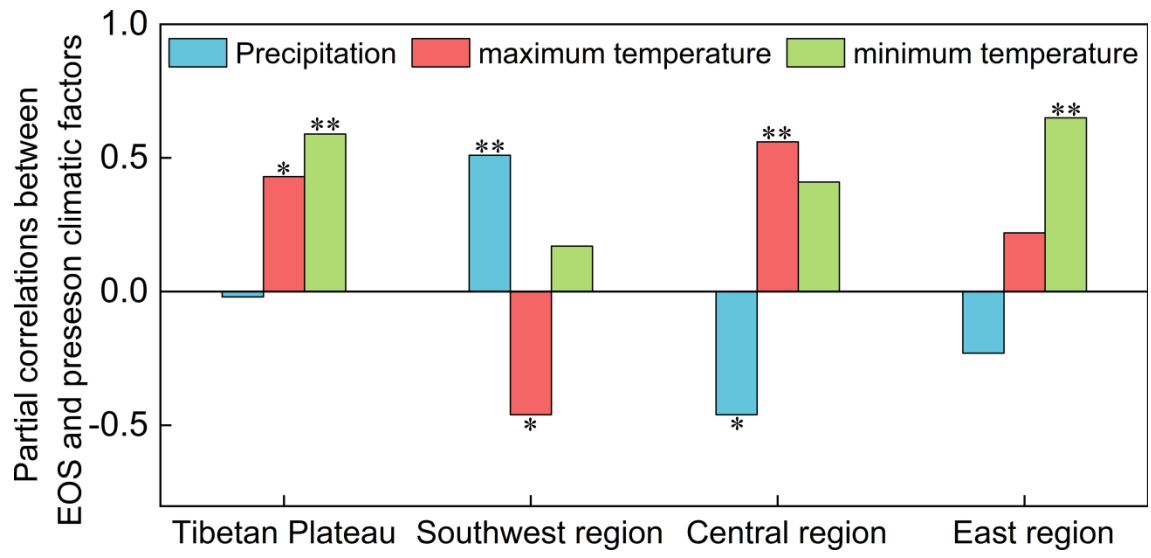
893



894

895

FIGURE 1

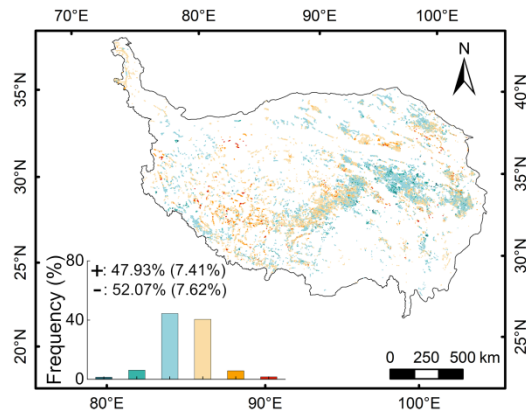


896

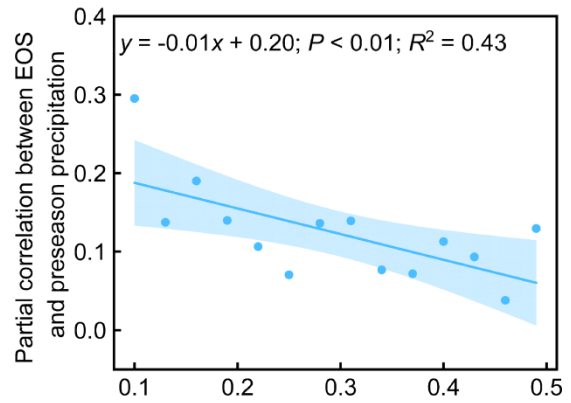
897

FIGURE 2

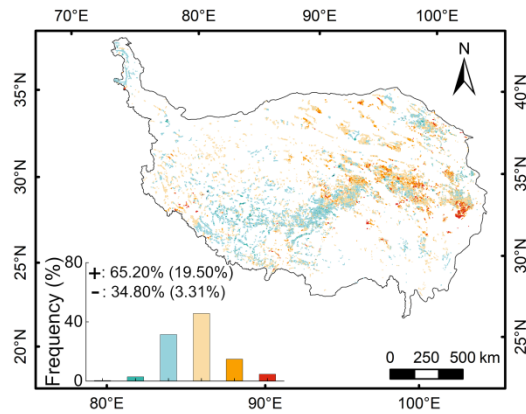
(a) EOS and pre-season precipitation



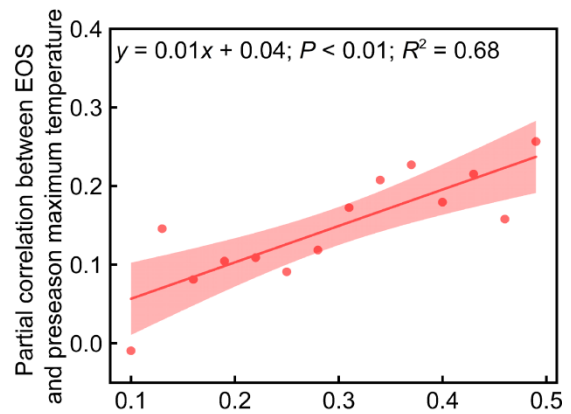
(b)



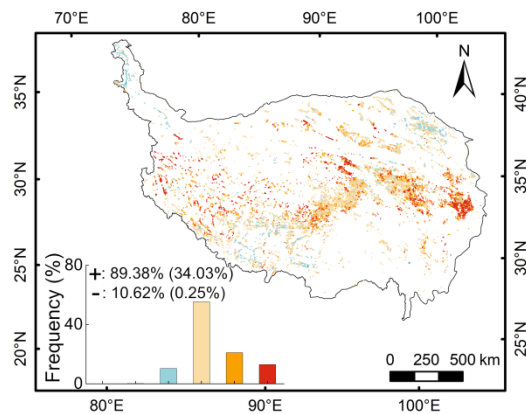
(c) EOS and pre-season maximum temperature



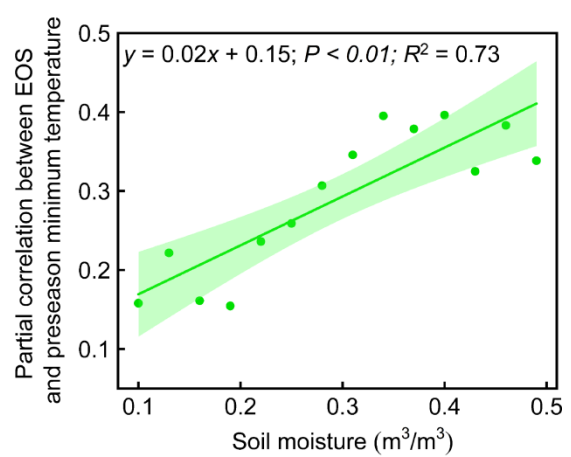
(d)



(e) EOS and pre-season minimum temperature



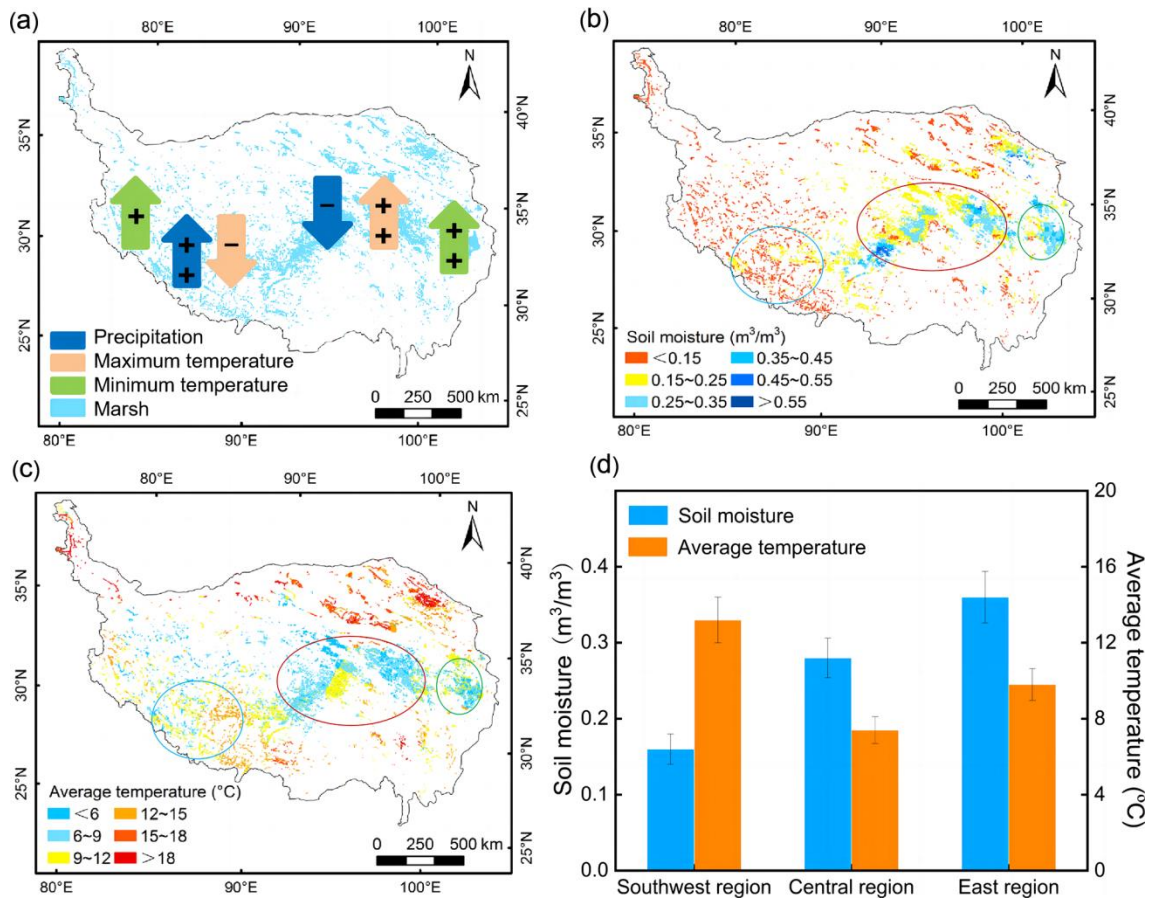
(f)



898

899

FIGURE 3

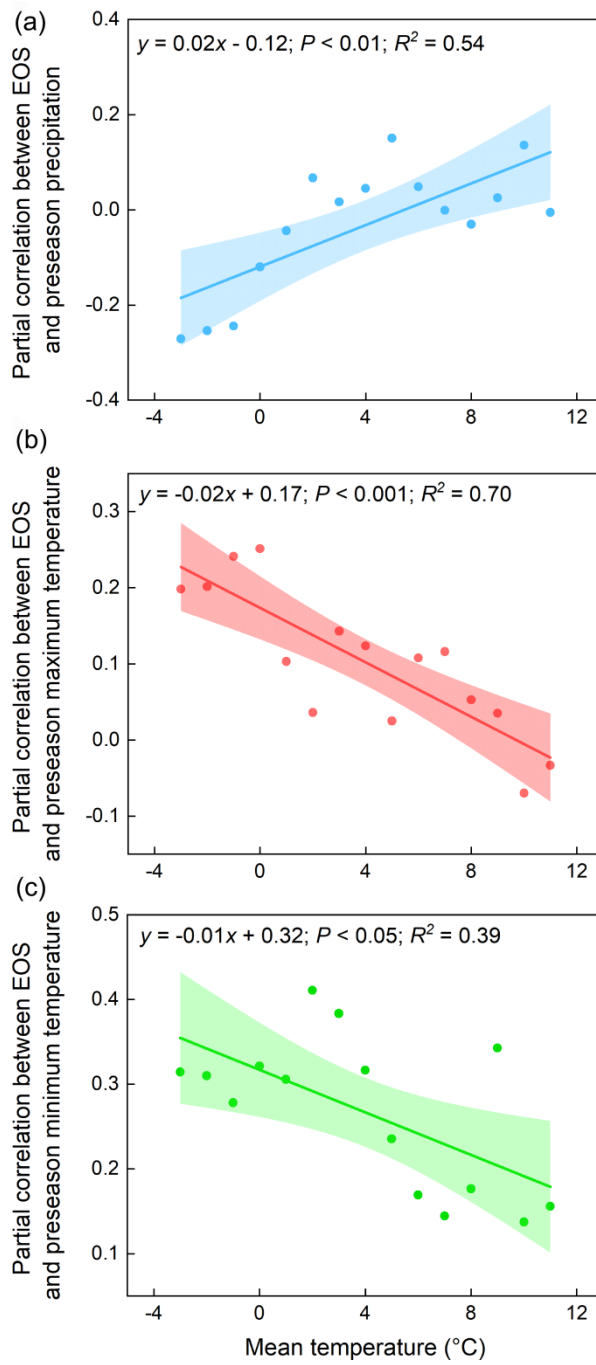


900

901

FIGURE 4



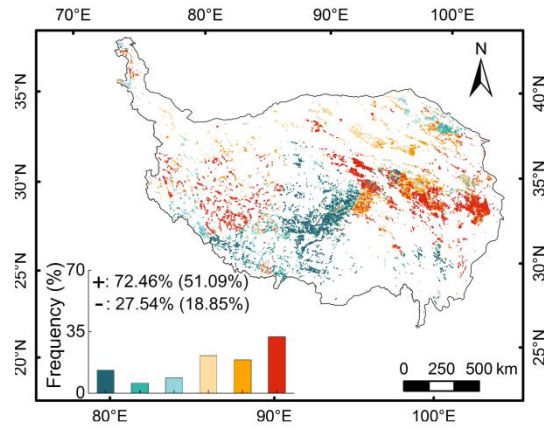


902

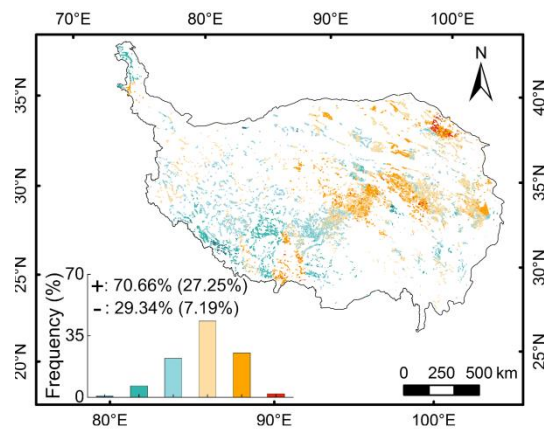
903

FIGURE 5

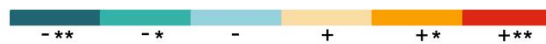
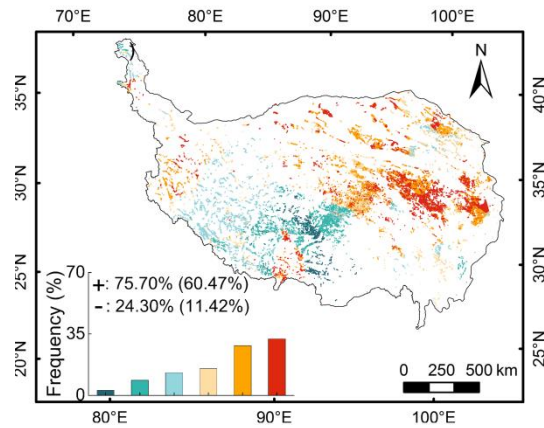
(a) Trend of pre-season precipitation (mm/a)



(b) Trend of pre-season maximum temperature ( $^{\circ}\text{C}/\text{a}$ )



(c) Trend of pre-season minimum temperature ( $^{\circ}\text{C}/\text{a}$ )



904

905

FIGURE 6